Fibers and Polymers 2019, Vol.20, No.9, 1766-1773
DOI 10.1007/s12221-019-8579-7

ISSN 1229-9197 (print version)
ISSN 1875-0052 (electronic version)

Thermal, Mechanical and Rheological Properties of Poly(lactic acid) Chain Extended with Polyaryl Polymethylene Isocyanate

Yanping Hao[1], Yi Li[1]*, Zhigang Liu[1], Xiangyu Yan[1], Yi Tong[1]*, and Huiliang Zhang[2]

[1]*National Engineering Research Center of Corn Deep Processing, Jilin COFCO Biochemistry Co., Ltd., Changchun 130033, China*

[2]*Key Laboratory of Polymer Ecomaterials, Chinese Academy of Sciences, Changchun Institute of Applied Chemistry, Changchun 130022, China*

(Received July 2, 2018; Revised March 5, 2019; Accepted April 19, 2019)

Abstract: In this study, polyaryl polymethylene isocyanate (PAPI) was used as a chain extender for poly(lactic acid) (PLA) to produce a high molecular weight material with better rheological, thermal and mechanical properties. The reaction between PLA chains and PAPI was proved by FTIR during reactive blending. The results showed that the molecular weight and molecular weight distribution were increased with the addition of PAPI content due to the chain extension. Chain extension was also responsible for the increased modulus and complex viscosity. The glass transition temperature (T_g) and thermal stability increased by incorporating with PAPI. The results of mechanical properties showed that a considerably higher tensile strength and Young's modulus of the reactive blends compared with neat PLA.

Keywords: Poly(lactic acid), Polyaryl polymethylene isocyanate, Rheological properties, Thermal behavior, Mechanical properties

Introduction

In recent years, biodegradable polymers have been received much more attention because of their potential applications in the fields related to environmental protection. Among these polymers, poly(lactic acid) (PLA) is one of the most important biodegradable and bio-based polymers [1]. It is a linear, aliphatic, thermoplastic polyester that are produced from either L-lactic acid or D-lactic acid monomers for useful applications [2]. These monomers are obtained through fermentation of corn starch, sugarcane juice or other agricultural resources [3,4]. PLA is commercially available in variety of grades and has been approved by the U.S. Food and Drug Administration (FDA) [5-7]. It has been extensively applied to biomedical fields such as absorbable sutures [8], drug-delivery systems [9], bone fixation parts [10], and tissue engineering scaffolds [11] because of its excellent biocompatibility, bioabsorbability, biodegradability, and good mechanical properties. PLA has also been increasingly used in food and industrial packaging [12]. Moreover, PLA has the potential to replace traditional petroleum-based plastics (e.g., polystyrene and polyethylene terephthalate) [14] in many disposable or short-term applications, such as disposable tableware, carrier bags, and agricultural mulch films due to its renewability, biodegradability, compostability, processibility, and transparency [12-16]. However, some of its physical properties, such as its toughness, dimensional stability, melt viscosity, crystallization rate, and gas barrier properties, are still not satisfactory for processing and application [17]. Consequently, there is a sustained interest in overcoming these disadvantages without a drastic loss in its general performance to meet various end-use applications.

To enlarge its processing window and applications field, PLA needs to be melt strengthened. Chain modification is the main reported way to obtain enhanced melt properties for PLA [18-22]. Chain extension is the reaction of functional molecules with the carboxyl or hydroxyl end groups of PLA chains. Chain extenders usually increase molecular weight of PLA by entering between two chain ends [23]. Bifunctional chain extenders can react with two end groups, which lead to a linear structure, whilst the multifunctional chain extenders with more than two functionalities result in branched or cross-linked structures [24,25]. The tailoring of this number allows the creation of specific chain structures as reported by Mihai *et al.* [26]. The active entities can be carboxylic, hydroxyl, peroxide, isocyanate or epoxide groups reacting with carboxyl or hydroxyl chain ends of PLA. Some of the chain extenders used in these studies are 1,6-diisocyanatohexane, 1,4-butanedioldiglycidylether, poly(phenyl isocyanate-co-formaldehyde), pyromellitic dianhydride, diepoxides, epoxydized acrylic copolymers, 1,4-phenylenebisoxazoline, and phatalicanhydride [27-31].

Zhong *et al*. used methylenediphenyl diisocyanate (MDI) as the chain extender for low molecular weight PLA [32]. The results showed that higher molecular weight and higher T_g of PLA could be obtained through the chain-extending reaction of the low molecular weight PLA with MDI and the heat resistance of PLA was improved. Corre *et al*. [20] used an epoxide additive (Joncryl ADR-4368) to melt strengthen the pristine PLA with the objective to enlarge its process-ability window. The rheological investigations highlighted the enhancement of the melt properties by using the chain

*Corresponding author: ly1964cofco@sina.com
*Corresponding author: tongyi1963@sina.cn

extender [33]. Najafi *et al*. [34] compared the thermal stabilization effects of TNPP, PCDI and Joncryl ADR-4368 and concluded that Joncryl ADR-4368 was the most efficient chain extender. The addition of 1 wt% Joncryl in PLA nanocomposites containing 2 wt% organo-modified clay improved the PLA thermal stability by a chain extension reaction, resulting in a long chain branched structure.

PAPI is a multifunctional crosslinking agent. In previous study, poly(propylene carbonate) (PPC) could be easily crosslinked using PAPI as a crosslinking agent [35]. The crosslinked PPC exhibited dramatically improved thermal and mechanical properties compared with uncrosslinked PPC.

In this study, PAPI was used as a chain extender of PLA. The effect of PAPI on the rheological, thermal and mechanical properties of PLA were investigated.

Experimental

Materials

PLA (4032D) used in this study comprising around 98 % L-lactide is a commercial product of Natureworks Co. Ltd., USA. It has molecular weight (M_w) of 250,000 g/mol and polydispersity of 1.70 (by GPC analysis). PAPI is provided by Jing Jiang City Special Adhesive Factory, China. The number average molecular weight (M_n) and functionality of PAPI are 280 g/mol and 2.7, respectively. The structures of PLA and PAPI are shown in Scheme 1.

Sample Preparation

Melt compounding of PLA with 0, 0.5, 1.0, 1.5, 2.0 wt% of PAPI was conducted using a Haake batch intensive mixer (Haake Rheomix 600, Karlsruhe, Germany). Prior to blending, PLA was dried in vacuum for 24 h at 60 °C. The two components were mixed at 190 °C for 5 min, with a screw speed of 50 rpm. After mixing, PLA and its blends were cut into small pieces and then were hot-pressed at 190 °C for 5 min followed by cold-press at room temperature to form the sheets with thickness of 1 mm. The compression molding steps were carried out carefully in order to obtain the same treatment for every sample. For convenience, the processed neat PLA and PLA/PAPI blends are, respectively, designated as neat PLA and PLA*x* in the following discussion, *x* representing the PAPI content (wt%) of the blends.

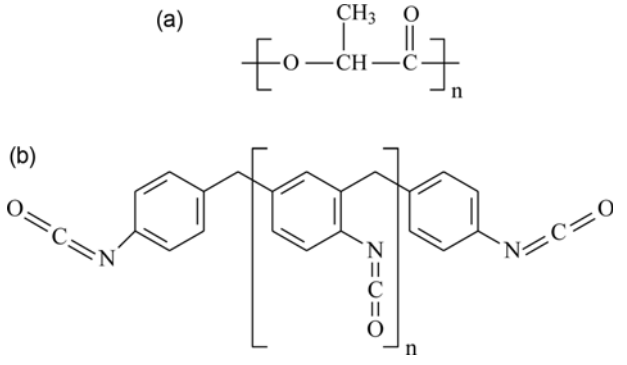

Scheme 1. Structures of PLA (a), and PAPI (b).

Characterization

Fourier transform infrared (FTIR) spectra was recorded with a Bruker Vertex 70 FTIR spectrometer (Bruker Instruments Co., Germany) using an attenuated total reflection (ATR) mode. The spectra within the range 4000-400 cm^{-1} with a resolution of 4 cm^{-1} and scan rate of 8 scans/s were observed.

The molecular weight parameters of PLA and its blends were measured by gel permeation chromatography (GPC) using a waters instrument (e2695 HPLC). GPC columns were eluted with THF at 25 °C at 1 m*l*/min according to DB22/T 2015-2014 standard.

Rheological measurements of the blends were conducted with the rheometer (TA Instruments Co., AR 2000ex, USA) at 185 °C. Frequency sweep for PLA and its blends was carried out under nitrogen using 25-mm plate-plate geometry. The thickness of sheet samples were about 1.0 mm. The gap distance between the parallel plates was 0.9 mm for all tests. The angular frequency range used during testing was 0.1-100 rad/s.

The T_gs of PLA and its blends were studied by dynamic mechanical analysis (DMA, TA Instruments Co., DMA, Q800, USA). The dimensions of the samples were 20 mm× 4 mm×1 mm. The experiment was carried out in tension mode at a constant heating rate of 3 °C/min from 20 to 100 °C and a frequency of 1 Hz.

Crystallization behaviors of PLA and its blends were studied by differential scanning calorimetry (DSC) (TA Instruments Co., DSC, Q20, USA) on the specimens sliced from compression molded samples. Samples (about 5-8 mg) were placed and sealed in aluminum pans. The samples were then heated first from 0 up to 180 °C at 10 °C/min (the first heating scan) and held at 180 °C for 3 min to eliminate their previous thermal history. Following that the samples were cooled to 0 °C at the same rate and then heated again to 180 °C at 10 °C/min (the second heating scan). The crystallinity of the samples was evaluated from the heat evolved during crystallization by the following relationship:

$$x_c = \frac{\Delta H_f}{w_{PLA} \times \Delta H_f^0} \times 100\% \quad (1)$$

where ΔH_f is the heat of fusion, ΔH_f^0 is the heat of fusion for 100 % crystalline PLA (93 J/g) [36] and W_{PLA} is the weight fraction of PLA.

The thermal stability of PLA and its blends was measured by thermogravimetric analysis (TGA, Perkin-Elmer TGA-7, USA). Neat PLA and the PLA/PAPI blends with weight of 10±0.2 mg were heated from room temperature to 600 °C at

10 °C/min under nitrogen.

The uniaxial tensile tests were carried out at room temperature on an 1121 testing machine (Instron Corporation, USA). Specimens (20 mm×4 mm×1 mm) were cut from the previously compression-molded sheet into a dumbbell shape. The measurements were conducted at a cross-head speed of 20 mm/min at room temperature according to ASTM D638-2008. At least five runs for each sample were measured, and the results were averaged.

Results and Discussion

FTIR Spectra

FTIR analysis provides important evidence for the reaction because it is sensitive and effective for structural characterization. The FTIR spectra of neat PLA, neat PAPI, and PLA2.0 were presented in Figure 1. It could be observed that the characteristic absorption at around 2275 cm^{-1} corresponded to the isocyanate groups (-NCO) characteristic absorption of PAPI disappeared for PLA2.0. Thus, it could be concluded that the active isocyanate groups of PAPI had been reacted with the hydroxyl end groups (-OH) of PLA. However, no new peaks appeared at the FTIR spectra for PLA2.0. Because of the low content of PAPI, there were no chemical groups could not been found in the FTIR spectra. The sharp absorption peak at 1748 cm^{-1} is typical for the C=O stretch of PLA, as shown in Figure 1.

Reaction Mechanism

It was reported that isocyanate groups could react with the hydroxyl end groups of PLA molecules through carbamate bonds [37], and the reaction of chain extension occurred as shown in Scheme 2(a). Because PLA had a very high molecular weight, terminal hydroxyl groups in the PLA was extremely low. The feed molar ratio of -NCO of PAPI to -OH of PLA was much higher than 1:1, and the excess amount of the isocyanate group might also react with the carboxylic

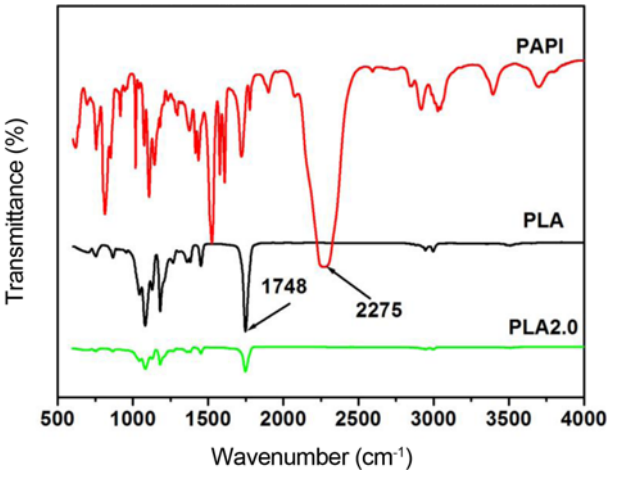

Figure 1. FTIR spectra of PLA, PAPI, and PLA2.0.

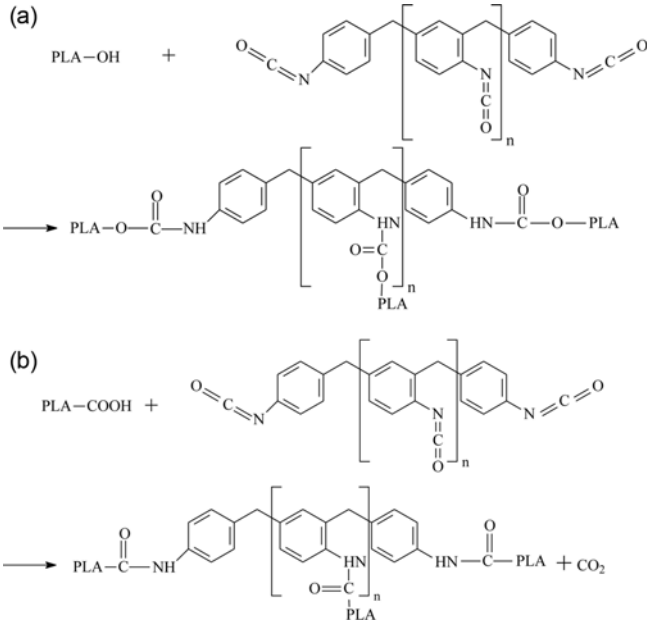

Scheme 2. Chain extension mechanism of PLA with PAPI; (a) reaction with hydroxyl ends groups and (b) reaction with carboxylic end groups.

end groups of PLA to form amide linkage according to reaction Scheme 2(b).

GPC Analysis

According to Yang *et al*. [38], the molecular weight of PLA generally decreased during melt processing, and also with increasing processing temperature. The molecular weight and distribution of PLA before and after addition of PAPI were characterized by GPC and the corresponding parameters were shown in Table 1. It could be observed that both the M_w and M_n of PLA increased with increasing PAPI content, which suggested that the isocyanate groups could react with the hydroxyl end groups of PLA. The excess amount of the isocyanate groups might also react with the carboxylic end groups of PLA molecule to form amide linkage to cause chain branching. The chain branching would widen the molecular weight distribution. That probably was the reason for the greater molecular weight distribution (PDI) of the chain-extended PLA than that of neat PLA, as listed in Table 1. However, the increment effect of PAPI on molecular weight of PLA was not so obvious. This might be because isocyanate reacted more easily with the carboxyl end group of PLA to form an amide linkage.

Rheology

Rheological behavior plays an important role in polymer processing. As it is known, foaming and film blowing especially require a relative high melt strength. The dynamic storage modulus (G') and loss modulus (G'') of PLA and its

Table 1. Relative molecular mass and its distribution of PLA before and after addition of PAPI

Sample name	M_n	M_w	MWD
PLA	180,087	242,330	1.35
PLA0.5	188,474	255,950	1.36
PLA1.0	192,999	263,413	1.36
PLA1.5	202,793	279,489	1.38
PLA2.0	211,514	291,634	1.38

blends obtained from the dynamic frequency sweep were shown in Figure 2. At high frequencies, the qualitative behaviors of G' and G'' were essentially similar and not affected by the existence of PAPI. However, G' and G'' increased monotonically with increasing PAPI content at low frequencies. The G' and G'' were also improved by means of the chain extension, suggesting that the extended structures could better withstand the shear strain as opposed to neat PLA. In addition, G'' was higher than G' over the entire frequency range, indicating the dominance of viscous responses over elastic responses.

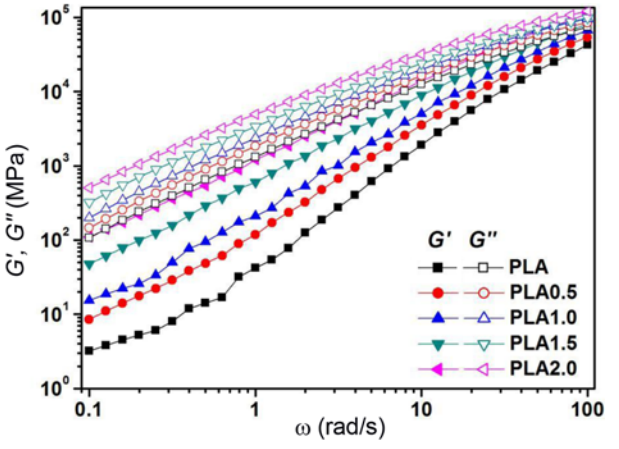

Figure 2. Plots of dynamic storage modulus (G') and loss modulus (G'') versus angular frequency (ω) for PLA and its blends.

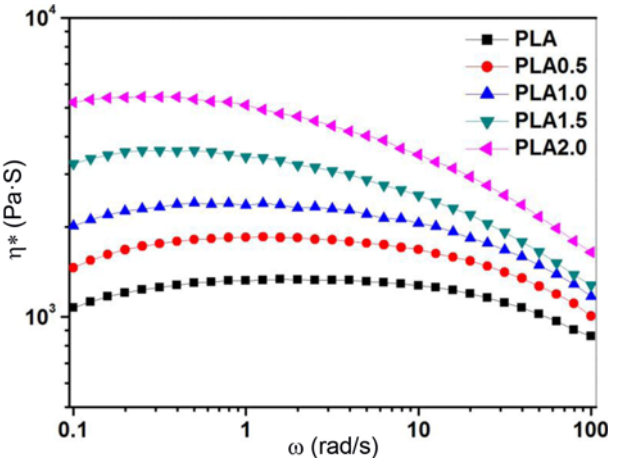

Figure 3. Plots of complex viscosity (η^*) versus angular frequency (ω) for PLA and its blends.

Figure 3 displayed the relationship between complex viscosity (η^*) and angular frequency (ω) of PLA and its blends. The η^* of neat PLA followed the general behavior of typical thermoplastic polymers, that is, near Newtonian behavior at low frequency and slight shear-thinning behavior at high frequency. With increasing PAPI content, it was clearly seen that the complex viscosity gradually increased, as shown in Figure 3. The increase in complex viscosity was related to the increase in the molecular weight of the polymers due to the reaction of chain extension between PLA and PAPI, as discussed in GPC analysis. In addition, with PAPI content increasing up to 1.5 wt%, the viscosity curve of the blends showed non-Newtonian shear thinning behavior, and no plateau regions was observed over the full frequency range.

The Han Analysis of Rheological Behavior

Figure 4 showed the Han plots of G'-G'' for PLA and its blends. The curves of the blends clearly presented PAPI content dependence. In addition, the reduced slope with the addition of PAPI indicated that the blends became more heterogeneous. It was notable that the inflection point where the slope was shifted to a higher frequency with increasing PAPI content. This indicated that much energy was necessary to change the degree of heterogeneity due to the increased physical association within the blends at a high content level. Those strong interactions between PLA and PAPI changed the relaxation behavior of the PLA chain inevitably. The relaxation time (λ) can be calculated as follows [39]:

$$\lambda = \frac{G'}{\eta^* \times \omega^2} \quad (2)$$

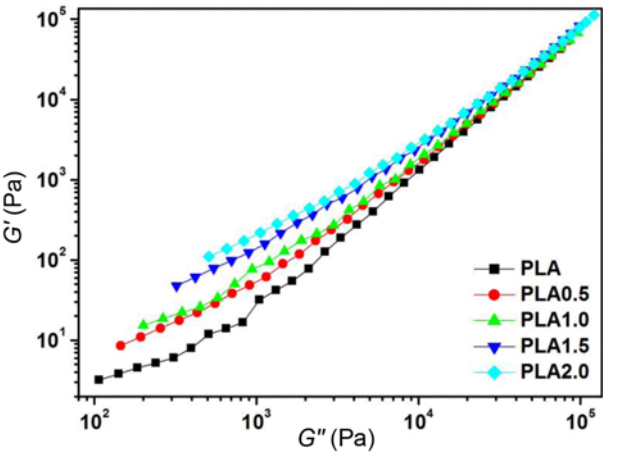

Figure 4. Han plots of dynamic storage modulus (G') versus dynamic loss modulus (G') at 190 °C for PLA and its blends.

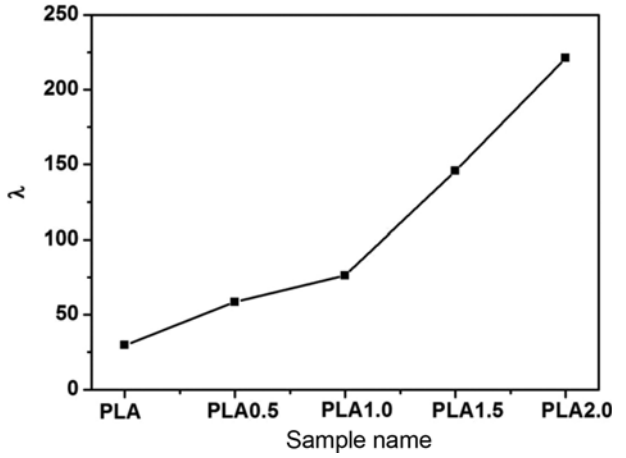

Figure 5. Plots of relaxation time (λ) versus PAPI content.

The calculated ratio of the relaxation time of PLA and its blends increased gradually with PAPI content at the low angular frequency (0.1 rad/s), as shown in Figure 5. It indicated that the addition of PAPI made the polymer chain need longer time for the relaxation became stronger. In other words, the presence of PAPI highly restricted the chain mobility of PLA.

DMA Analysis

Figure 6 showed the plots of loss storage (E'') as a function of temperature for PLA and its blends. The peak temperature corresponded to the glass transition temperature (T_g) of the sample. It could be seen that the T_g shifted to higher temperature as PAPI content increased, and the T_g of the blends increased from 58.3 °C for neat PLA to 63.4 °C for PLA1.5. However, a further increase of PAPI content, the T_g changed slightly. There might be two reasons for the elevation of T_g. On the one hand, the increment of the molecular weight reduced the number of free chain ends and thus reduced the free volumes [40,41]. On the other hand, the introduction of a rigid aromatic structure into the polymer chain hinders the chain movement sterically. From the DMA results, it could be concluded that the heat resistance of PLA could be improved by chain extending with PAPI.

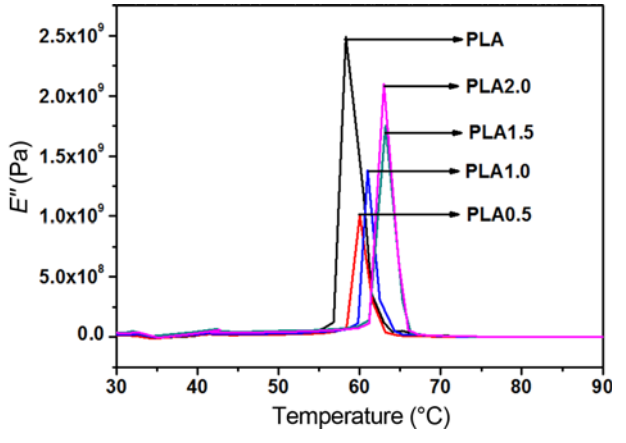

Figure 6. DMA traces of PLA and its blends at various concentrations: loss modulus (E'') versus temperature curve.

Crystallization Behaviors

Figure 7 showed the DSC second heating traces of PLA and its blends and the corresponding parameters were listed in Table 2. As shown in Figure 7, neat PLA showed an obvious glass transition temperature (T_g) at 62.1 °C and two melting temperatures of about 163.0 and 169.5 °C. In addition, an exothermic peak was presented corresponding to its cold crystallization at 111.8 °C. It could be seen that with the addition of PAPI, T_g was almost unchanged and only small differences existed within 1 °C. The T_g data obtained from DSC characterization were slightly different from DMA analysis. This was resulted from different test methods used.

The cold crystallization temperature (T_{cc}) of the blend was significantly different from that of neat PLA. Neat PLA represented a narrow exothermic peak at 111.8 °C. However, in the case of PLA/PAPI blends, this peak was broader and appeared at much higher temperature, and the crystallization enthalpies decreased correspondingly (Table 2). These results suggested that the incorporation of PAPI weakened the cold crystalline ability of PLA. By careful analysis, it was easy to detect that T_{cc} increased to the highest 119.4 °C with 1.0 wt% PAPI content. When the content of PAPI continued to increase, T_{cc} followed and shifted to the lower temperature. The ΔH_{cc} gradually decreased corresponded to the increase in PAPI content.

Furthermore, neat PLA showed two melting peaks in Figure 7, and the T_{m2} peak was preponderant in comparison with the T_{m1} peak. The phenomenon of the double melt

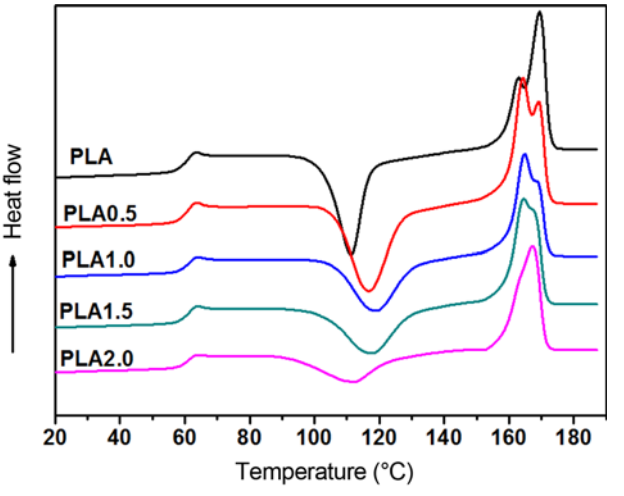

Figure 7. DSC second heating traces of PLA and its blends.

Table 2. Thermal and crystalline properties of PLA and its blends

Sample name	T_g (°C)	T_{cc} (°C)	ΔH_{cc} (J/g)	T_{m1} (°C)	T_{m2} (°C)	ΔH_f (J/g)	X_c (%)	T_{onset} (°C)
PLA	61.0	111.8	32.6	163.0	169.5	41.6	44.7	345.8
PLA0.5	61.4	116.5	39.6	164.3	169.4	43.5	47.0	346.1
PLA1.0	61.6	119.4	28.7	164.9	168.6	32.7	35.5	346.4
PLA1.5	61.9	118.0	28.5	164.5	167.5	35.9	39.2	351.8
PLA2.0	61.5	112.2	17.5	-	167.4	33.2	36.4	358.4

peaks was attributed to a melt recrystallization-remelting process upon heating. The lower temperature peak was ascribed to the melting of primary crystals and the higher temperature peak or shoulder corresponded to the melting of the recrystallized crystals [42-46]. In the case of the blends, the location of the two melting peaks was almost the same with that of neat PLA. However, significant change could be observed in the shape of the melting peaks of PLA with the addition of PAPI. The T_{m1} peak became preponderant in comparison with the T_{m2} peak with the addition of PAPI. It could be noted that the melting temperature of the higher peak gradually decreased with the increased PAPI content in the blend. The lower peak disappeared when PAPI content was 2.0 wt%, indicating the formation of crystallites was more perfected in the blend.

Thermal Stability

TGA curves for PLA and its blends under nitrogen were shown in Figure 8 and the corresponding data were summarized in Table 2. All of the blends gave reasonably stable thermal residues, which corresponded well with the PAPI contents. Thermal decomposition temperature for the blends significantly shifted to higher temperature range than that for neat PLA, and the decomposition temperature was strongly dependent on the PAPI content. The temperature corresponding to the onset of decomposition (T_{onset}) for a polymer is essential for evaluating its thermal stability and guiding melt processing. According to the data in Table 2, T_{onset} for the blends gradually increased with increasing PAPI content. For example, PLA2.0 exhibited the highest T_{onset} (358.4 °C), which was shifted approximately 13 °C towards higher temperature compared to neat PLA. This improvement in the thermal stability could be attributed to the longer polymer chains produced in the blends containing the chain extenders, and hence the reduced number of chain ends per mass.

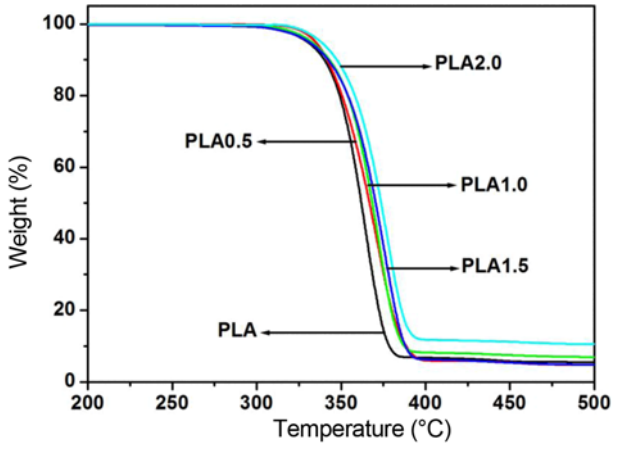

Figure 8. TGA curves of PLA and its blends under nitrogen obtained at a heating rate of 10 °C/min.

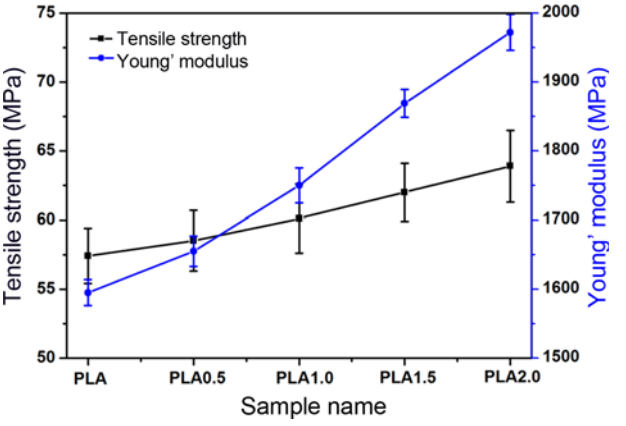

Figure 9. Tensile strength and Young's modulus of PLA and its blends.

Mechanical Properties

The tensile strength and Young's modulus for PLA and its blends were shown in Figure 9. The tensile strength and Young's modulus of the blends gradually increased with increasing PAPI content. For example, the tensile strength and Young's modulus increased from 57.4 MPa and 1595 MPa for neat PLA to 63.9 MPa and 1927 MPa for PLA2.0, as shown in Figure 9. The increase in these properties might be related to PLA molecular weight increased due to PLA chain extension and the formation of a long chain branching structure [47,48].

Conclusion

The current study investigated the chain extender effect on the rheological behavior, as well as on the thermal and mechanical properties of PLA. From the results of FTIR, it could be deduced that chain extension was occurred due to

the reaction between PLA and PAPI. The addition of PAPI increased the molecular weight and molecular weight distribution of PLA. The results of rheological analysis showed that the modulus and complex viscosity in the melt state of the blends were increased compared with that of neat PLA due to the chain extension. The T_g shifted to higher temperature as PAPI content increased, and the T_g of the blend increased from 58.3 °C for neat PLA to 63.4 °C for PLA1.5. In particular, the introduction of PAPI resulted in the improvement of thermal stability. PLA with 2.0 wt% PAPI exhibited the highest T_{onset} (358.4 °C), which is shifted approximately 13 °C towards higher temperature compared to neat PLA. Upon increasing content of PAPI, the blends showed increased tensile strength and Young's modulus.

Acknowledgments

This study was supported by the fund of Science and Technology Bureau of Jilin Province of China (No. 20170204012SF) and the project National of Key Research and Development Program of China (No. 2016YFC0501402).

References

1. A. Sodergard and M. Stolt, *Prog. Polym. Sci.,* **27**, 1123 (2002).
2. Z. Xiong, X. Y. Dai, H. N. Na, Z. B. Tang, R. Y. Zhang, and J. Zhu, *J. Appl. Polym. Sci.,* **132**, 41220-1 (2015).
3. K. Magniez, A. S. Voda, A. A. Kafi, A. Fichini, Q. Guo, and B. L. Fox, *ACS Appl. Mater. Interf.,* **5**, 276 (2013).
4. K. Oksman, M. Skrifvars, and J. F. Selin, *Compos. Sci. Technol.,* **63**, 1317 (2003).
5. R. A. Jain, *Biomaterials*, **21**, 2475 (2000).
6. A. GMikos, M. D. Lyman, L. E. Freed, and R. Langer, *Biomaterials*, **15**, 55 (1994).
7. T. G. Park, S. Cohen, and R. Langer, *Macromolecules*, **25**, 116 (1992).
8. R. Auras, B. Harte, and S. Selke, *Macromol. Biosci.,* **4**, 835 (2004).
9. Y. M. Zhao, Z. Y. Wang, J. Wang, H. Z. Mai, B. Yan, and F. Yang, *J. Appl. Polym. Sci.,* **91**, 21 (2004).
10. K. M. Nampoothiri, N. R. Nair, and R. P. John, *Bioresour. Technol.,* **101**, 8493 (2010).
11. M. Okamoto and B. John, *Prog. Polym. Sci.,* **38**, 1487 (2013).
12. S. Saeidlou, M. A. Huneault, H. B. Li, and C. B. Park, *Prog. Polym. Sci.,* **37**, 1657 (2012).
13. R. M. Rasal, A. V. Janorkar, and D. E. Hirt, *Prog. Polym. Sci.,* **35**, 338 (2010).
14. V. P. Martino, A. Jiménez, R. A. Ruseckaite, and L. Avérous, *Polym. Adv. Technol.,* **22**, 2206 (2011).
15. M. P. Arrieta, J. López, S. Ferrándiz, and M. A. Peltzer, *Polym. Test.,* **32**, 760 (2013).
16. R. E. Drumright, P. R. Gruber, and D. E. Henton, *Adv. Mater.,* **12**, 1841 (2000).
17. X. Wen, Y. Lin, C. Y. Han, K. Y. Zhang, X. H. Ran, Y. S. Li, and L. S. Dong, *J. Appl. Polym. Sci.,* **114**, 3379 (2009).
18. P. R. Gruber, M. H. Hartmann, J. J. Kolstad, D. R. Witzke, and A. L. Brosch, Method of Crosslinking PLA. PCT 94/08 508.
19. J. Tuominen, J. Kylmä, and J. Seppälä, *Polymer*, **43**, 3 (2000).
20. D. Yingwei, I. Salvatore, M. Ernesto Di, and N. Luigi, *Macromol. Mater. Eng.,* **290**, 1083 (2005).
21. S. Pilla, S. G. Kim, G. K. Auer, S. Gong, and C. B. Park, *Polym. Eng. Sci.,* **49**, 1653 (2009).
22. M. Mihai, M. A. Huneault, and B. D. Favis, *Polym. Eng. Sci.,* **50**, 629 (2010).
23. T. Basak and O. Guralp, *J. Polym. Environ.,* **25**, 983 (2017).
24. S. Pilla, A. Kramschuster, L. Yang, J. Lee, S. Gong, and L. S. Turng, *Mater. Sci. Eng.,* **29**, 1258 (2009).
25. Y. M. Corre, A. Maazouz, J. Duchet, and J. Reignier, *J. Supercrit. Fluids.,* **58**, 177 (2011).
26. M. Mihai, M. A. Huneault, and B. D. Favis, *Polym. Eng. Sci.,* **50**, 629 (2010).
27. P. Raffa, M. B. Coltelli, S. Savi, S. Bianchi, and V. Castelvetro, *React. Funct. Polym.,* **72**, 50 (2012).
28. F. Awaja and D. Pavel, *Eur. Polym. J.,* **41**, 2614 (2005).
29. L. Incarnato, P. Scarfato, L. D. Maio, and D. Acierno, *Polymer*, **41**, 6825 (2000).
30. G. P. Karayannidis and E. A. Psalida, *J. Appl. Polym. Sci.,* **77**, 2206 (2000).
31. D. N. Bikiaris and G. P. Karayannidis, *J. Polym. Sci. Part A: Polym. Chem.,* **34**, 1337 (1996).
32. W. Zhong, J. J. Ge, Z. Y. Gu, W. J. Li, X. Chen, Y. Zang, and Y. L. Yang, *J. Appl. Polym. Sci.,* **74**, 2546 (1999).
33. Y. M. Corre, J. M. Duchet, J. Reignier, and A. Maazouz, *Rheol. Acta.,* **50**, 613 (2011).
34. N. Najafi, M. C. Heuzey, P. J. Carreau, and M. Wood-Adams, *Polym. Degrad. Stabil.,* **97**, 554 (2012).
35. Y. P. Hao, H. H. Ge, L. J. Han, H. Y. Liang, H. L. Zhang, and L. S. Dong, *Polym. Bull.,* **70**, 1991 (2013).
36. Z. Su, Q. Li, Y. Liu, G. Hu, and C. Wu, *Eur. Polym. J.,* **45**, 2428 (2009).
37. X. Li, H. Kang, J. Shen, L. Zhang, T. Nishi, K. Ito, C. Zhao, and P. Coates, *Polymer*, **55**, 4313 (2014).
38. L. X. Yang, X. S. Chen, and X. B. Jing, *Polym. Degrad. Stabil.,* **93**, 1923 (2008).
39. D. F. Wu, L. Wu, M. Zhang, and Y. L. Zhao, *Polym. Degrad. Stabil.,* **93**, 1577 (2008).
40. K. Hiltunen, J. V. Seppala, and M. Harkonen, *J. Appl. Polym. Sci.,* **63**, 1091 (1997).
41. J. Kylma, M. Harkonen, and J. V. Seppala, *J. Appl. Polym. Sci.,* **63**, 1865 (1997).
42. J. Zhang, K. Tashiro, H. Tsuji, and A. J. Domb, *Macromolecules*, **41**, 1352 (2008).
43. M. Yasuniwa, K. Sakamo, Y. Ono, and W. Kawahara,

Polymer, **49**, 1943 (2008).
44. P. Pan, W. Kai, B. Zhu, T. Dong, and Y. Inoue, *Macromolecules*, **40**, 6898 (2007).
45. P. Pan, Z. Liang, B. Zhu, T. Dong, and Y. Inoue, *Macromolecules*, **42**, 3374 (2009).
46. T. Kawai, N. Rahman, G. Matsuba, K. Nishida, T. Kanaya, M. Nakano, H. Okamoto, J. Kawada, A. Usuki, N. Honma, K. Nakajima, and M. Matsuda, *Macromolecules*, **40**, 9463 (2007).
47. J. Liu, L. Lou, W. Yu, R. Liao, R. Li, and C. Zhou, *Polymer*, **51**, 5186 (2010).
48. M. P. Grosvenor and J. N. Staniforth, *Int. J. Pharm.,* **135**, 103 (1996).